# Influence of electronic structure and multiexciton spectral density on multiple-exciton generation in semiconductor nanocrystals: Tight-binding calculations

G. Allan and C. Delerue*

*Département ISEN, Institut d'Electronique de Microélectronique et de Nanotechnologie (UMR CNRS 8520), 41 Boulevard Vauban, F-59046 Lille Cedex, France*

(Received 30 November 2007; revised manuscript received 7 February 2008; published 27 March 2008)

Several experimental works have reported that a single high-energy photon could generate multiple excitons in semiconductor nanocrystals and several theories have been proposed to explain these results. Using a tight-binding method, we calculate the electronic structure of InAs, Si, and PbSe nanocrystals and we investigate two models of the multiple exciton generation (MEG). We show that the impact ionization process is efficient at high energy, with lifetimes as small as 10 fs. The behavior of the impact ionization rate versus the energy is basically the same in all materials in spite of large differences in their electronic structure. We present simulations of the MEG showing that, in PbSe and Si nanocrystals, the impact ionization alone cannot explain the efficiencies measured at high energy, even in the limit where there is no relaxation of the excited carriers by electron-phonon scattering. In InAs nanocrystals, the impact ionization process could only explain the lowest yields reported in the literature. We calculate the spectral densities of multiexciton states and we evaluate the possibility of direct and instantaneous photogeneration of multiexcitons. We confirm the importance of the multiexciton spectral densities in the MEG problem because of their rapid variation over several orders of magnitude as a function of the energy. However, we show that the high MEG efficiencies in PbSe and Si nanocrystals, up to seven excitons per photon, would imply a very efficient relaxation in multiexciton states, whereas they are characterized by a negligible density.

DOI: 10.1103/PhysRevB.77.125340 PACS number(s): 73.22.Dj, 78.67.Hc, 71.35.−y, 71.15.−m

## I. INTRODUCTION

When photons of energy $h\nu$ are absorbed in a bulk semiconductor of band gap $\varepsilon_g$, a large part of the excess energy $h\nu-\varepsilon_g$ is converted into heat due to the thermalization of the carriers by electron-phonon scattering. This effect strongly limits the efficiency of conventional solar cells. Recently, it was claimed that this limitation could be overcome in semiconductor nanocrystals due to the formation of multiexcitons by carrier multiplication.[1,2] The multiple exciton generation (MEG), if efficient, could boost the applications of nanocrystals in the field of solar energy conversion.

Efficient MEG was first reported in PbSe and PbS nanocrystals[1,3,4] and was later observed in CdSe nanocrystals.[5,6] More recently, it was also measured in InAs (Refs. 7 and 8) and Si nanocrystals.[9] All these results suggest that the phenomenon is general to nanocrystalline materials in spite of large differences in their electronic structure. However, the origin and even the existence of an efficient MEG in nanocrystals remain largely discussed. Recent measurements by transient photoluminescence spectroscopy on CdSe and CdTe nanocrystals[10] have found no evidence for MEG in deep contrast to previous reports.[6] A complete theory has yet to explain the efficiency of MEG which seems to be incompatible with the experiments showing that excited carriers efficiently cool by phonon relaxation.[11–14] It is also intriguing that, at high photon energy, the number of generated excitons is often close to the absolute maximum imposed by the energy conservation rule (equal to the integer part of $h\nu/\varepsilon_g$).[5]

Several models have been proposed to interpret the experiments. The simplest process which could be at the origin of the MEG is the impact ionization, when an excited carrier decays to a lower-energy state and its energy is transferred to create an extra electron-hole pair.[1] Indeed, tight-binding[15] and pseudopotential[16] calculations predict fast relaxation of excited carriers by impact ionization in PbSe and PbS nanocrystals, with lifetimes smaller than 1 ps in a wide range of energy.[15] However, we have presented simulations of the relaxation process in PbSe and PbS nanocrystals, showing that an efficient impact ionization is not sufficient to explain the observed MEG yields at high energy ($h\nu>3\varepsilon_g$).[15] Two effects explain this result. First, after the absorption of a photon of energy $h\nu$, the excess energy $h\nu-\varepsilon_g$ is distributed between the electron and the hole. Second, the relaxation energy in the impact ionization process is in average larger than $\varepsilon_g$, which tends to reduce the excess energy available for the remaining carriers. Therefore, the extremely high yields (up to 700%) (Ref. 4) experimentally obtained can be only explained if there are other mechanisms of energy transfer between the excited particles (beyond the simple impact ionization process) which tend to optimize the number of excitons.

The analysis of the exciton population dynamics indicates that the MEG is almost an instantaneous event,[4] which is also difficult to reconcile in the mechanism of impact ionization. Thus, two models have been proposed, in which the multiexciton states are directly photogenerated. In the first model, single-exciton states are coupled to multiexciton states via virtual single-exciton states (second-order perturbation theory).[4] In the second model, the authors consider a coherent superposition of all the excitonic states of same energy.[17] Even if these two models shed new light on the MEG problem, there are not conclusive because of their approximations,[10] in particular, they consider a simplified electronic structure of the nanocrystals and they do not cal-

 

culate all the Coulomb matrix elements at the origin of the coupling between the excitonic states.

In this paper, our objective is to discuss several points related to the influence of the electronic structure on the MEG. We study nanocrystals of three semiconductors (PbSe, Si, and InAs) with very different band structures, and we compare these systems on the basis of tight-binding calculations. PbSe is a IV-VI semiconductor characterized by a cubic rocksalt lattice and a narrow band gap at the $L$ point of the Brillouin zone. Si and InAs have a zinc-blende lattice, but they differ by the nature of their gap, i.e., indirect for Si and direct for InAs.

In the first part of the paper, we study the impact ionization process in Si and InAs nanocrystals, complementing our work on PbSe and PbS nanocrystals.[15] We show that the behavior of the impact ionization lifetime versus the energy of the excited carriers is basically the same in all the materials because it is mainly governed by the density of final states like in PbSe nanocrystals.[15,16] We simulate the MEG when the impact ionization is in competition with the relaxation by electron-phonon scattering. We obtain that the impact ionization certainly contributes to the MEG but, in Si nanocrystals, cannot explain the observed yields at high ratio $h\nu/\varepsilon_g$; once again, in line with our results on PbSe and PbS.[15] We also discuss the case of InAs nanocrystals where quite different experimental results have been recently published.[7,8]

In the second part of the paper, we consider the direct photogeneration of multiexciton states, as proposed in Refs. 4 and 17. In these models, the efficiency of the MEG is mainly governed by two types of factors: (1) the dephasing and relaxation rates of the multiexcitons for which there is no proper description in nanocrystals;[10,17,18] and (2) the multiexciton spectral densities that recent papers have pointed out the important role.[4,15–17,19] References 4 and 17 suggested that the dynamics of the carriers at high energy $h\nu$ could be explained by a strong coupling of single-exciton states to resonant multiexciton ones by Coulomb interactions. In these conditions, the system would naturally evolve to multiexciton states if their spectral density is high and if the carrier relaxation is not too fast in the single-exciton states. We suppose that the probability to find the excited system in a $n$-exciton state is approximately given by

$$p_n(h\nu) = \frac{N_n(h\nu)}{\Sigma_n N_n(h\nu)}, \tag{1}$$

where $N_n(h\nu)$ is the spectral density of $n$-exciton states at the excitation energy $h\nu$. In that case, the average exciton multiplicity is given by $\langle N_x(h\nu)\rangle = \Sigma_n n p_n(h\nu)$. Thus, our objective is to evaluate the possible role of multiexciton spectral densities in the MEG. We present calculations of these quantities in PbSe, Si, and InAs nanocrystals. We obtain that the spectral densities have a common behavior with a marked threshold and a variation over many orders of magnitude, which confirms their importance in the problem. We calculate the average exciton multiplicity $\langle N_x(h\nu)\rangle$ and we show that it does not coincide with the observed yields of MEG. We conclude that the experiments cannot be explained only by the relative weights of the multiexciton spectral densities, but that other processes must be also considered. We show that, in PbSe nanocrystals, at the energies where very high efficiencies of the MEG are reported (up to 700%),[4] the states corresponding to these high multiplicities have a negligible density. Implications of our results are discussed.

TABLE I. Diameter ($d$) and energy gap ($\varepsilon_g$) of the nanocrystals considered in this work.

| | $d$ (nm) | $\varepsilon_g$ (eV) |
|---|---|---|
| Si | 2.7 | 2.1 |
| Si | 3.4 | 1.84 |
| PbSe | 1.9 | 1.89 |
| PbSe | 3.1 | 1.19 |
| InAs | 3.0 | 1.75 |
| InAs | 3.8 | 1.52 |
| PbSe | 2.5 | 1.52 |

## II. IMPACT IONIZATION

### A. Methodology

The impact ionization rate in InAs and Si nanocrystals is obtained using the same method as in our previous work on PbSe nanocrystals.[15] First, we calculate the electronic structure of the nanocrystals in tight-binding calculations to determine the single-particle states and energies. Details on the method are described elsewhere for PbSe,[20] InAs,[21] and Si.[22] The size and energy gap of the nanocrystals considered in this work are shown in Table I. Second, we consider an excited carrier of energy $\varepsilon$, either a hole in the valence band ($\varepsilon<0$, the zero energy corresponding to the top of the bulk valence band) or an electron in the conduction band ($\varepsilon>0$). The impact ionization rate is given by the Fermi golden rule as

$$W(\varepsilon) = 2\pi|V(\varepsilon)|^2\rho_f(\varepsilon)/\hbar, \tag{2}$$

where $V(\varepsilon)$ is the transition matrix element of the screened Coulomb interaction and $\rho_f(\varepsilon)$ is the density of final states, in which the carrier has relaxed and an extra electron-hole pair is created. The energy being conserved in the impact ionization process, $W(\varepsilon)$ vanishes when the carrier excess energy is smaller than $\varepsilon_g$ [the carrier excess energy is equal to $\varepsilon-\varepsilon_c$ for an electron and $\varepsilon_v-\varepsilon$ for a hole, where $\varepsilon_c$ ($\varepsilon_v$) is the lowest (highest) conduction (valence) level of the nanocrystal]. A broadening of 5 meV of each peak in $\rho_f(\varepsilon)$ is used to simulate the coupling of the electronic states to their environment, in particular, to the phonons.[18]

### B. Results and discussion

#### 1. Impact ionization lifetime

The evolution of the impact ionization lifetime $[1/W(\varepsilon)]$ with the energy $\varepsilon$ of the carrier is shown in Fig. 1 for Si and InAs nanocrystals. Quite similar results were obtained in PbSe and PbS nanocrystals.[15] As expected, there is an energy

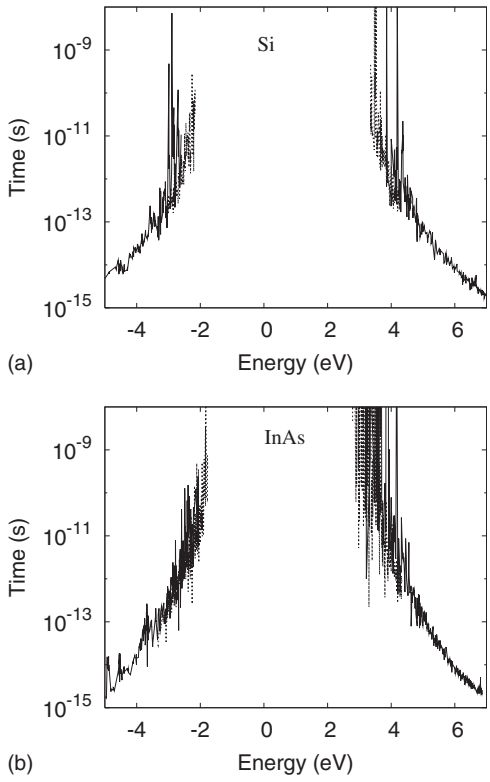


FIG. 1. Impact ionization lifetime $(1/W)$ versus the energy $\varepsilon$ of the carrier in (a) Si and (b) InAs nanocrystals (solid line: diameter=2.7 nm for Si and 3.0 nm for InAs and dotted line: 3.4 nm for Si and 3.8 nm for InAs). The curves for different sizes strongly overlap each other. The zero of energy corresponds to the top of the bulk valence band.

window around the gap, in which the impact ionization is not allowed and its width increases with the confinement. Outside this window, the curves are almost independent of the nanocrystal size. Near the thresholds, there are strong oscillations of the impact ionization lifetime due to the scarcity of the resonant states, as a consequence of the quantum confinement. This effect is particularly important in the conduction band of InAs nanocrystals [$\varepsilon > 0$ in Fig. 1(b)] because the conduction band minimum is nondegenerate in InAs and is characterized by a small effective mass leading to large confinement energies. The oscillations were less visible in the case of PbSe nanocrystals (Fig. 2 of Ref. 15) because of the high multiplicity of the conduction and valence band extrema.

Figure 2 reveals that the matrix element $V(\varepsilon)$ is almost constant as function of $\varepsilon$, except close to the thresholds. Therefore, the evolution of the impact ionization rate with respect to the carrier energy $\varepsilon$ is mainly governed by the density of final states $\rho_f(\varepsilon)$ [given in Fig. 1(b) of Ref. 15 for PbSe]. We have verified that $V(\varepsilon)$ is also nearly constant in the case of InAs and Si. These results justify the approximation of a constant matrix element used in Ref. 16, except just above the thresholds.

### *2. Multiple exciton generation induced by the impact ionization*

Figure 1 shows that the impact ionization lifetime can be extremely short at high carrier excess energy, in the tens of

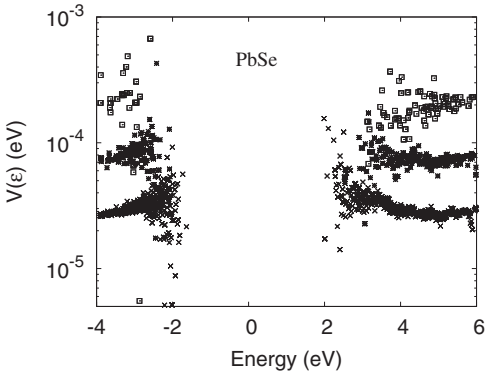


FIG. 2. Matrix elements $V(\varepsilon)$ of the screened Coulomb interaction involved in the impact ionization [Eq. (2)] versus the energy $\varepsilon$ of the excited carrier in PbSe nanocrystals of diameter of 1.9 nm (⊡), 2.5 nm (*), and 3.1 nm (×). In practice, we calculate the average of the matrix elements over all the final states in an energy window of 1 meV around $\varepsilon$.

femtosecond range, like in the case of PbSe and PbS.[15,16] Our results prove that this conclusion does not depend on the nature of the semiconductor. In order to evaluate the contribution of the impact ionization to the MEG, we have numerically simulated the MEG, resulting from the following successive processes: (1) the optical absorption that determines the distribution of energies of the electron and the hole and (2) the relaxation either by impact ionization or by emission of phonons. We simulate the relaxation step by step, until complete relaxation of all the generated carriers. The methodology is described in our previous work.[15] We assume that the lifetime for the relaxation by electron-phonon scattering is a constant $\tau_{ph}$ independent of the energy, but we present the results for different values of $\tau_{ph}$. In Fig. 3, we plot the number $P(h\nu)$ of generated excitons per nanocrystal and per absorbed photon. With reasonable values of $\tau_{ph}$ in the $10^{-13}$–$10^{-12}$ s range, we see that $P(h\nu)$ reaches values well above one exciton, either in PbSe, Si, or InAs nanocrystals. We deduce that the contribution of the impact ionization to the observed MEG is probably non-negligible. In Ref. 10, the authors found no evidence of MEG in CdSe and CdTe nanocrystals even when the excitation energy $h\nu$ exceeds $3\varepsilon_g$. From our work, this would imply a lifetime $\tau_{ph}$ smaller than 10 fs, at least at high carrier excess energy. Therefore, accurate determinations of intraband relaxation lifetimes in nanocrystals are needed to conclude.

An interesting result of our simulations of the impact ionization process in Si [Fig. 3(b)] and PbSe [Fig. 3(a) and Fig. 5 of Ref. 15] nanocrystals is that $P(h\nu)$ underestimates the observed MEG yields at high energy, not only for reasonable values of $\tau_{ph}$ but also for $\tau_{ph} \to \infty$. We have also calculated $P_{max}(h\nu)$, i.e., the maximum number of excitons that could be created by impact ionization after excitation of an electron-hole pair. $P_{max}(h\nu)$ is given by $1+P_e+P_h$, where $P_e$ $(P_h)$ is the integer part of the excess energy of the electron (hole) divided by the gap energy $\varepsilon_g$.[15] Figure 3(b) shows that the experimental yields in Si nanocrystals are higher than the calculated values of $P_{max}(h\nu)$ at high energy. We conclude that the impact ionization alone cannot explain the experi-

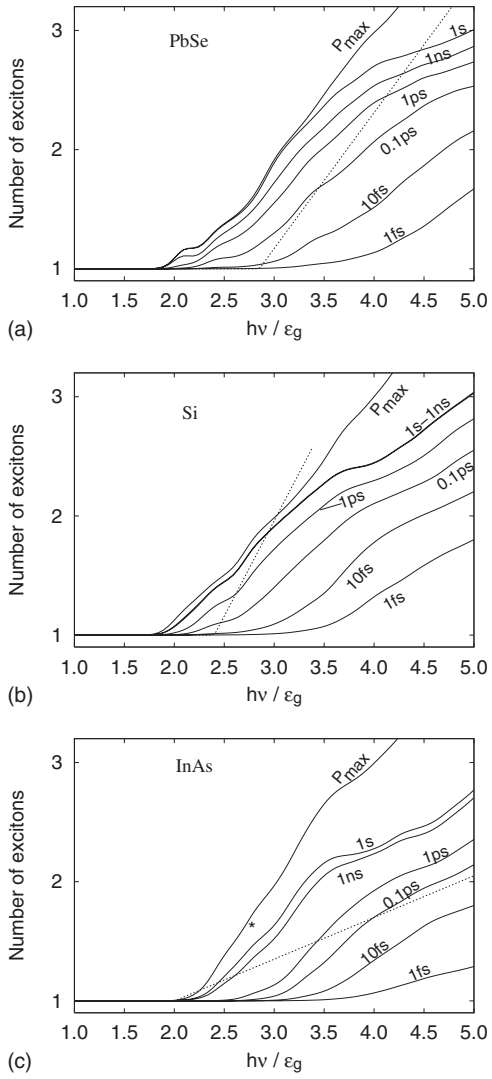


FIG. 3. Full lines: calculated number of excitons obtained by impact ionization as a function of the pump photon energy normalized by $\varepsilon_g$ in (a) PbSe (diameter=3.1 nm), (b) Si (diameter =2.7 nm), and (c) InAs (diameter=3.0 nm) nanocrystals. $P_{\max}$ is the maximum number of excitons which could be obtained by impact ionization with electron and hole energies determined by the absorption process; the other curves correspond to the full simulation $[P(h\nu)]$ for different values of the lifetime $\tau_{\rm ph}$ for the relaxation by phonon emission. The dotted lines represent experimental yields: results of Ref. 4 for PbSe (a), of Ref. 9 for Si (b), and of Ref. 8 for InAs (c) (⋆: result of Ref. 7). The results for PbSe (a), already shown in Ref. 15, are reproduced here for comparison.

mental results in PbSe and Si nanocrystals, even in the absence of relaxation by phonon emission.

The case of InAs nanocrystals [Fig. 3(c)] must be separately discussed because the two experimental studies published on this system report rather different MEG yields. In Ref. 7, ~1.6 excitons are obtained per absorbed photon at $\sim 2.7\varepsilon_g$. Figure 3(c) shows that it represents a high value, close to $P_{\max}(h\nu)$, and well above our simulations, even for $\tau_{\rm ph}=1$ s. At $2.7\varepsilon_g$, Ref. 8 reports a lower value (~1.2) which could be obtained in our simulations with $\tau_{\rm ph}\approx 0.1$ ns. Also, compared to PbSe and Si, a lower threshold near $2\varepsilon_g$ is measured. Above this threshold, a linear growth of the MEG efficiency is observed, with a slope of $\sim 35\%/\varepsilon_g$ instead of $\sim 100\%/\varepsilon_g$ in PbSe (Ref. 4) and CdSe,[5] and $\sim 150\%/\varepsilon_g$ in Si.[9] As a consequence of the smaller slope in InAs nanocrystals, the experimental efficiencies above $\sim 3\varepsilon_g$ are close to the theoretical values calculated with $\tau_{\rm ph}\approx 0.1-1$ ps [Fig. 3(c)]. Therefore, the measurements of Ref. 8 could be explained in the impact ionization model if we assume that the relaxation rate strongly depends on the carrier energy, which is a possible situation due to the confinement effects which are more important at lower exciton energy.

## III. GENERATION OF MULTIEXCITONS

In order to explain the high MEG efficiencies in PbSe and Si nanocrystals, it is necessary to take into account other mechanisms, such as a strong coupling of the multiexciton states together.[4,15,17] In the following, we consider the extreme case where all multiexciton states at a given energy are so efficiently coupled by Coulomb interactions that the system is capable to explore all of them before relaxation (we leave out the question whether this process is coherent[17] or not[4]). In this situation, it is reasonable to suppose that the system will naturally relax in the multiexciton states which have the higher density at the excitation energy $h\nu$.[19] Thus, we have calculated $N_n(h\nu)$, i.e., the spectral density of the $n$-exciton states, as a function of $h\nu$ and for different values of $n$ (up to 6).

### A. Methodology

We consider all the states with $n$ excitons, i.e., with $n$ electrons in the conduction states $(\{\varepsilon_c^i\}, i=1\cdots n)$ and $n$ holes in the valence states $(\{\varepsilon_v^i\}, i=1\cdots n)$. The excitation energy is $\varepsilon_c^1-\varepsilon_v^1$ for the first exciton, $\varepsilon_c^2-\varepsilon_v^2$ for the second one, etc. Therefore, the total excitation energy is equal to $\Sigma_{i=1}^n[\varepsilon_c^i-\varepsilon_v^i]$ and the spectral density $N_n(h\nu)$ is given by

$$N_n(h\nu)=\sum_{\{\varepsilon_c^i\},\{\varepsilon_v^i\}}\delta\left(h\nu-\sum_{i=1}^{n}[\varepsilon_c^i-\varepsilon_v^i]\right), \tag{3}$$

where the sum is over all the possible configurations with $n$ electrons and $n$ holes, excluding the situations where the Pauli exclusion principle is not verified. We broaden each delta function by a Gaussian of full width at half maximum of $0.047\varepsilon_g$. In Eq. (3), the multiexciton energies are evaluated using single-particle energies, neglecting interparticle Coulomb and exchange couplings. We will discuss this point later and in Appendix A. Because the calculations require heavy computational resources, the spectral densities are calculated in the limited range of energy necessary to perform the following calculations.

In order to quantify the MEG in this model and to compare to experiments, we have calculated the average multiplicity $\langle N_x(h\nu)\rangle$ of photogenerated excitons from the spectral densities of multiexciton states. Following Schaller and Klimov,[19] we write $\langle N_x(h\nu)\rangle=\Sigma_n np_n(h\nu)$. From Eq. (1), we obtain

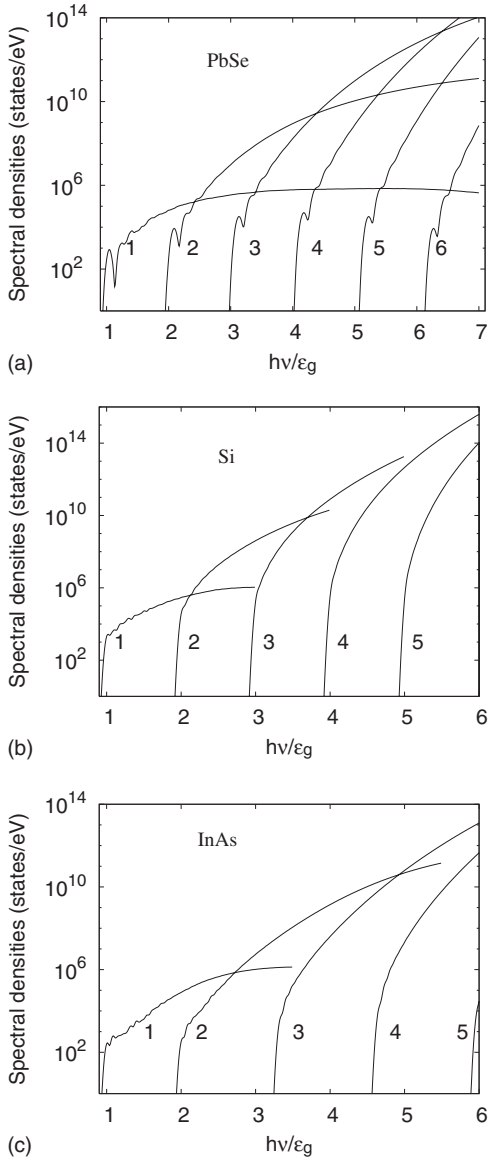


FIG. 4. Spectral densities $N_n(h\nu)$ of $n$-exciton states versus the excitation energy $h\nu$ in (a) PbSe, (b) Si, and (c) InAs nanocrystals (diameters of 3.1, 3.4, and 3.8 nm, respectively). The multiplicity $n$ is indicated for each curve. The nonzero density below the thresholds is just an effect of the broadening used in the calculations.

$$\langle N_x(h\nu)\rangle = \frac{\Sigma_n n N_n(h\nu)}{\Sigma_n N_n(h\nu)}. \quad (4)$$

### B. Results and discussion

#### 1. Spectral densities of multiexciton states

Figure 4 shows the spectral densities in PbSe, Si, and InAs nanocrystals, calculated from Eq. (3). The overall behavior is the same in the three materials. The most striking feature of the spectral densities is their variation over several orders of magnitude because there is an increasing number of ways of distributing the energy between $n$ excitons.[15,16] This effect is particularly visible in a simple model which assumes a constant density of single-particle states (Appendix B).

$N_n(h\nu)$ presents a sharp increase with energy just above a threshold determined by the energy conservation and the Pauli exclusion principle. This threshold is close to $n\varepsilon_g$ for all investigated values of $n$ in PbSe and Si nanocrystals, but only for $n=1$ and $n=2$ in InAs nanocrystals where the thresholds for $n \geqslant 3$ are shifted to higher energy. This distinct behavior is due to the twofold degeneracy of the lowest empty state in InAs nanocrystals, while there is a manifold of 12 and 16 states in Si (Ref. 22) and PbSe (Ref. 20) nanocrystals, respectively, due to the higher multiplicity of their conduction band minima (intervalley splittings are not visible at the scale considered here).

In spite of the sharp increase above their respective threshold, $N_n(h\nu)$ and $N_{n+1}(h\nu)$ do not intersect at the energy $(n+1)\varepsilon_g$, but at a higher energy that we denote $\varepsilon(n|n+1)$. The position of the intersection points depends on the shape of the spectral densities, thus on the nature of the semiconductor. However, the difference $\varepsilon(n|n+1)-(n+1)\varepsilon_g$ always strongly increases with $n$. For example, the intersect between $N_2(h\nu)$ and $N_3(h\nu)$ takes place above $4\varepsilon_g$ in PbSe [Fig. 4(a)], thus we expect a number of photogenerated excitons at maximum equal to 3 for $h\nu < 4\varepsilon_g$.

#### 2. Average multiplicity of excitons in PbSe nanocrystals

Figure 5(a) shows the average multiplicity $\langle N_x(h\nu)\rangle$ in a PbSe nanocrystal calculated from Eq. (4). $\langle N_x(h\nu)\rangle$ is a smoothed staircase function of the excitation energy, with a step at each energy $\varepsilon(n|n+1)$. This shape could be expected from the behavior of the functions $N_n(h\nu)$. In addition, $\langle N_x(h\nu)\rangle$ presents a sharp threshold just above $h\nu/\varepsilon_g=2$ and overestimates the experimental yields for $h\nu/\varepsilon_g \lesssim 3.8$.[4] On the contrary, at higher energy, $\langle N_x(h\nu)\rangle$ clearly underestimates the experimental values.[4] A MEG efficiency of 600% is reported at $h\nu/\varepsilon_g \approx 7$, which implies that the system is able to relax into states with six excitons whereas, at the same energy, there is a much higher density of states with four or five excitons [Fig. 4(a)]. In the picture of coherent superposition of multiexciton states,[17] this means that the system decays (decoheres) into states with a much lower density, which requires a very efficient process. This would be possible for example if the relaxation by electron-phonon scattering is much faster in states with six excitons than with four or five excitons, which remains to be proven (but this point was discussed in Ref. 17).

In order to see how the relaxation rate should depend on the multiplicity to interpret the experimental data, we use a new expression for the probability of a $n$ multiplicity ($\gamma_1 = 1$),

$$\tilde{p}_n(h\nu) = \frac{\gamma_n N_n(h\nu)}{\Sigma_n \gamma_n N_n(h\nu)}, \quad (5)$$

and for the average multiplicity,

$$\langle \tilde{N}_x(h\nu)\rangle = \sum_n n\tilde{p}_n(h\nu) = \frac{\Sigma_n n\gamma_n N_n(h\nu)}{\Sigma_n \gamma_n N_n(h\nu)}. \quad (6)$$

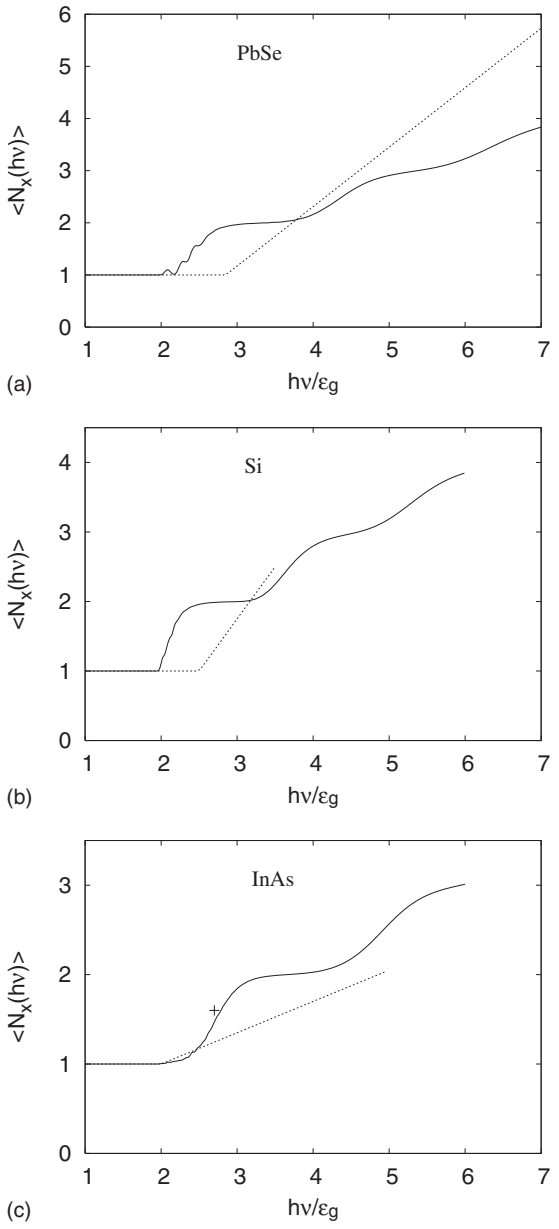


FIG. 5. Average multiplicity of excitons $\langle N_x(h\nu)\rangle$ determined from the spectral densities $N_n(h\nu)$ using Eq. (4) in PbSe (a), Si (b), and InAs (c) nanocrystals (diameters of 3.1, 3.4, and 3.8 nm, respectively). The dotted lines are the experimental MEG yields of Ref. 4 for PbSe, Ref. 9 for Si, and Ref. 8 for InAs (+: result of Ref. 7).

The coefficients $\gamma_n$ are parameters (Table II) that we adjust to fit $\langle \tilde{N}_x(h\nu)\rangle$ on the variations of the experimental MEG yields with excitation energy. The amplitude of these coefficients gives an idea of the relative strength of the relaxation processes in each excitonic channel needed to explain the experiments. In the case of PbSe nanocrystals [Fig. 6(a)], a linear variation and an excellent fit can be obtained. Interestingly, with these parameters (Table II), the probabilities $\tilde{p}_n(h\nu)$ have a remarkable peaked shape (Fig. 7) that closely resembles to the one deduced by Schaller and Klimov[19] from experiments. In that case, the intersects between the functions $\gamma_n N_n(h\nu)$ are distributed at a regular interval close to $\varepsilon_g$.

TABLE II. Coefficients $\gamma_n$ used to adjust the average multiplicity $\langle \tilde{N}_x(h\nu)\rangle$ on the experimental MEG yields ($\gamma_1=1$). In the case of Si and InAs, only $\gamma_2$ and $\gamma_3$ are adjusted due to the limited range of energy in which the MEG yields have been measured.

| | $\gamma_2$ | $\gamma_3$ | $\gamma_4$ | $\gamma_5$ | $\gamma_6$ |
|---|---|---|---|---|---|
| PbSe | 0.01 | 0.02 | 3 | $10^4$ | $5\times10^8$ |
| Si | 0.01 | 0.2 | 3 | $10^4$ | $5\times10^8$ |
| InAs | 0.01 | $2\times10^{-4}$ | 3 | | |

#### 3. Average multiplicity of excitons in Si nanocrystals

The results for $\langle N_x(h\nu)\rangle$ and $\langle \tilde{N}_x(h\nu)\rangle$ in Si nanocrystals are presented in Figs. 5(b) and 6(b), respectively. Like in PbSe, $\langle N_x(h\nu)\rangle$ is too high compared to experiments for $h\nu/\varepsilon_g \lesssim 3.2$ and is too small above. Good agreement with experiments is obtained with $\langle \tilde{N}_x(h\nu)\rangle$, in which $\gamma_2$ and $\gamma_3$ are fitted parameters (Table II). The coefficients $\gamma_4$, $\gamma_5$, and $\gamma_6$ cannot be derived because the MEG yield in Si nanocrystals has been measured in a smaller energy scale ($h\nu/\varepsilon_g < 3.4$) than in PbSe due to the larger band gap of Si.[9] So, we kept the same values for $\gamma_4$, $\gamma_5$, and $\gamma_6$ as for PbSe, just to visualize possible trends at higher energy. The fitted curve reproduces the high experimental slope of $\sim 150\%/\varepsilon_g$,[9] which requires a coefficient $\gamma_3$ higher than in PbSe (0.2 instead of 0.02). Above $h\nu/\varepsilon_g \approx 3.4$, a smaller slope is expected in average; otherwise, the MEG efficiency would exceed the maximum imposed by the energy conservation.

#### 4. Average multiplicity of excitons in InAs nanocrystals

As previously discussed, the case of InAs nanocrystals [Figs. 5(c) and 6(c)] is distinct from PbSe and Si. $\langle N_x(h\nu)\rangle$ is already in good agreement with the value of ~1.6 excitons per absorbed photon at $h\nu/\varepsilon_g \approx 2.7$ reported in Ref. 7. Also, we have found that it is more difficult to fit $\langle \tilde{N}_x(h\nu)\rangle$ to the experimental values of Ref. 8 because it is impossible to get at the same time a threshold at $h\nu/\varepsilon_g \approx 2$ and a slope of $\sim 35\%/\varepsilon_g$. The small slope requires to reduce the values of $\gamma_2$ and $\gamma_3$, which tends to shift the threshold to higher energy. A typical example is shown in Fig. 6(c).

#### 5. Discussion

The comparison between the different materials shows that the coefficients $\gamma_n$ are not universal (Table II). However, clear trends can be seen. The coefficients $\gamma_2$ and $\gamma_3$ are smaller than 1, which means that either the relaxation is more efficient in single-exciton states than in biexciton and triexciton states or the system has a small probability to go from single-exciton states to biexciton states before relaxation by electron-phonon scattering. The latter case corresponds to the model discussed in Sec. II, where the impact ionization process is in competition with the phonon cooling. We believe that it is the likely situation at low energy (for

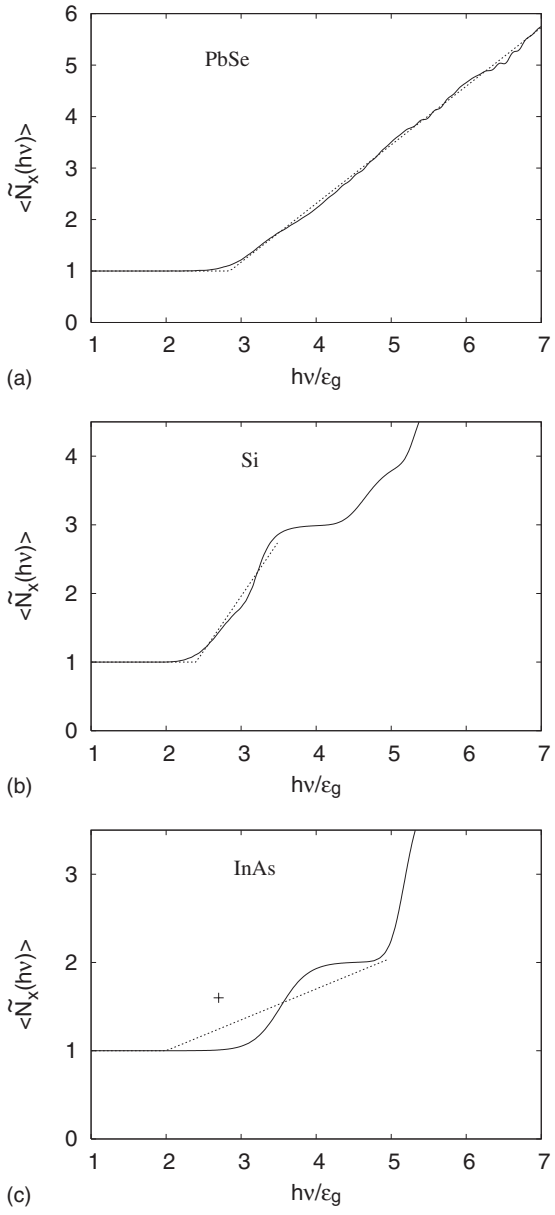


FIG. 6. Average multiplicity of excitons $\langle \tilde{N}_x(h\nu) \rangle$ in (a) PbSe (diameter=3.1 nm), (b) Si (diameter=3.4 nm), and (c) InAs (diameter=3.8 nm) nanocrystals determined from the spectral densities $N_n(h\nu)$ using Eq. (6) and the coefficients $\gamma_n$ of Table II. Dotted lines: experimental MEG yields of Ref. 4 for PbSe, Ref. 9 for Si, and Ref. 8 for InAs (+: result of Ref. 7).

example $h\nu/\varepsilon_g \lesssim 3.5$) by taking into account our results of Figs. 1 and 3, showing that the impact ionization is probably not sufficiently efficient compared to the relaxation by phonon emission. The position of the threshold in PbSe and Si nanocrystals well above $h\nu/\varepsilon_g = 2$ supports this conclusion.

The situation at higher energy ($h\nu/\varepsilon_g \gtrsim 3.5$) is different since the coupling of single-exciton states to multiexciton states probably becomes competitive compared to the phonon relaxation (Fig. 3). If the system can be in a superposition of multiexciton states, our results show that it is important to consider the rapid variation of their densities with the energy. In the case of PbSe nanocrystals, we deduce from the

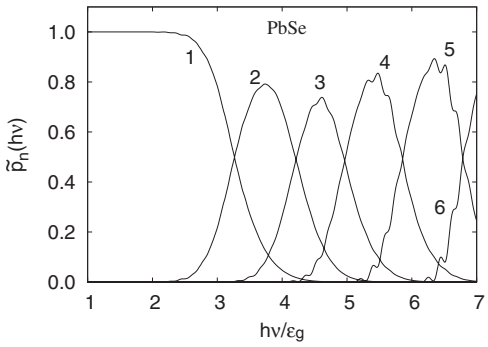


FIG. 7. Spectral distribution of the probabilities $\tilde{p}_n(h\nu)$ to find the system in a $n$-exciton state (PbSe nanocrystal, diameter =3.1 nm). The exciton multiplicity $n$ is indicated for each curve.

simulations that coefficients $\gamma_4$, $\gamma_5$, and $\gamma_6$ larger than 1 and varying over several decades are needed to interpret the experimental MEG efficiencies. In particular, $\gamma_5$ and $\gamma_6$ are higher than $\gamma_2$ by 6 and 10 orders of magnitudes, respectively, which seems to be unrealistic. We conclude that the high MEG efficiencies in PbSe nanocrystals cannot be explained in this model either.

Finally, we believe that all these conclusions would not be altered if we include interparticle Coulomb interactions in the calculations. The reasons are discussed in Appendix A.

## IV. CONCLUSION

In conclusion, we have performed calculations of the electronic structure of PbSe, Si, and InAs nanocrystals to study the generation of multiple excitons which has been reported in several experimental works. In the first part of the paper, we have considered the impact ionization process and we obtain that its rate strongly varies with the energy, following closely the behavior of the density of final states, in which the relaxation of the carrier has induced the creation of an extra electron-hole pair. In all the materials, we predict impact ionization lifetimes as low as 10 fs at high excess energy of the carriers, but we show that it is not sufficient to explain the highest MEG efficiencies measured in PbSe and Si nanocrystals. This conclusion may differ in the case of InAs nanocrystals if the lower MEG efficiencies are experimentally confirmed.

In the second part of the paper, we have considered a model in which, after photoexcitation, the system is in a superposition of multiexciton states. In that case, the densities of multiexciton states play an important role in the problem due to their rapid variation with the energy over several orders of magnitude. If there is superposition of multiexciton states, the experimental results on PbSe and Si nanocrystals can be only understood if the decay rate is smaller in the biexciton and triexciton states than in single-exciton states. On the contrary, at higher photon energy, the high yields reported in PbSe nanocrystals cannot be explained in this model because they would require extremely efficient decay processes in five- and six-exciton states whereas, comparatively, they are characterized by a negligible density at these

energies. Our work shows that measurements of the MEG efficiency at higher energy could be interesting in Si and InAs nanocrystals to settle the mechanism of direct photogeneration of multiexcitons. Also, other models like the one recently presented by Rupasov and Klimov[23] should be considered in future works. Finally, we confirm the need to have a better knowledge of phonon-assisted relaxation processes as a function of the carrier energy.

## APPENDIX A: INTERPARTICLE INTERACTIONS IN MULTIEXCITON STATES

All calculations that we have performed are based on the independent particle approximation. In this appendix, we estimate the effects of interparticle interactions on the multiexciton spectral densities. We show that they do not modify the conclusions of the paper. In principle, electron-electron, hole-hole, and electron-hole interactions could be described by using a multiconfiguration interaction technique. This type of calculation has been used to study the lowest states of single excitons,[18,24–26] but it requires heavy computational resources and becomes inapplicable for high energy multiexciton states. However, we consider nanocrystals in the strong confinement regime, meaning that quantum confinement effects dominate over correlation effects. The total wave function of the excited system can be approximately written as a product—or as a Slater determinant—of single-particle states and we have just to calculate the total energy as an average of the Hamiltonian in this configuration.[18,27] For a $n$-exciton state, the total energy of excitation with respect to the ground state is given by

$$E_{\mathrm{exc}}^{n} \approx \varepsilon_{\mathrm{exc}}^{n} + \langle \Sigma \rangle + \langle E_{\mathrm{Coul}} \rangle, \tag{A1}$$

where $\varepsilon_{\mathrm{exc}}^{n}$ is the single-particle energy of the $n$-exciton state [given by $\sum_{i=1}^{n}(\varepsilon_{c}^{i}-\varepsilon_{v}^{i})$ in Eq. (3)], $\langle \Sigma \rangle$ is the total self-energy correction,[18,28] and $\langle E_{\mathrm{Coul}} \rangle$ is the average of the screened Coulomb interactions between all (quasi)particles in this configuration. Equation (A1) only contains the main corrections to the single-particle energy.[18,21] Previous works based on $GW$ calculations[28] showed that the self-energy term is mainly given by the interaction between the charge carriers and the polarization charges induced by their own presence in the nanocrystal and can be safely calculated using classical electrostatic theory, in which the nanocrystal is described by its dielectric constant $\epsilon_{\mathrm{in}}$. By separating the contributions coming from the $n$ holes ($h$) and $n$ electrons ($e$), Eq. (A1) can be rewritten as

$$E_{\mathrm{exc}}^{n} \approx \varepsilon_{\mathrm{exc}}^{n} + n\Sigma_{e} + n\Sigma_{h} + V_{ee} + V_{hh} + V_{eh}, \tag{A2}$$

where $\Sigma_{e}$ ($\Sigma_{h}$) is the self-energy correction for one electron (hole), $V_{ee}$ ($V_{hh}$) is the interelectron (hole) Coulomb interaction energy, and $V_{eh}$ is the contribution coming from the electron-hole interactions. All these quantities have already been estimated in the case of single excitons using the single-particle wave-function $\sin(\pi r/R)/r$ of effective mass theory and these approximations have been justified by more elaborate calculations.[18,28–30] By assuming the same wave function for all the particles, the average of the screened Coulomb interaction between two electrons (or two holes) is given by[18,29,30]

$$V_{\mathrm{Coul}} = 1.79\frac{e^{2}}{\epsilon_{\mathrm{in}}R} + \frac{\alpha_{eh}(\epsilon_{\mathrm{in}}-\epsilon_{\mathrm{out}})}{R}, \tag{A3}$$

where $\alpha_{eh}=e^{2}/(\epsilon_{\mathrm{in}}\epsilon_{\mathrm{out}})$ and $\epsilon_{\mathrm{out}}$ is the dielectric constant of the material surrounding the nanocrystal. We deduce the interaction energies between the $n$ electrons and $n$ holes,

$$V_{ee} = V_{hh} = \frac{n(n-1)}{2}V_{\mathrm{Coul}}. \tag{A4}$$

$$V_{eh} = -n^{2}V_{\mathrm{Coul}}. \tag{A5}$$

The self-energies are given by[18,30] $\Sigma_{e}=\Sigma_{h}=\alpha_{1}(\epsilon_{\mathrm{in}}-\epsilon_{\mathrm{out}})/(2R)$, where

$$\alpha_{1} = \frac{e^{2}}{\epsilon_{\mathrm{in}}\epsilon_{\mathrm{out}}} + \frac{0.933e^{2}}{\epsilon_{\mathrm{in}}(\epsilon_{\mathrm{in}}+\epsilon_{\mathrm{out}})} - \frac{0.376e^{2}\epsilon_{\mathrm{out}}}{\epsilon_{\mathrm{in}}(\epsilon_{\mathrm{in}}+\epsilon_{\mathrm{out}})^{2}}. \tag{A6}$$

By injecting these quantities into Eq. (A2), we obtain that the correction to the single-particle energy for a $n$-exciton system is just equal to $n$ times the single-exciton binding energy $E_{\mathrm{BX}}$,

$$E_{\mathrm{exc}}^{n} - \varepsilon_{\mathrm{exc}}^{n} \approx -nE_{\mathrm{BX}}$$

$$E_{\mathrm{BX}} = \left[1.79\frac{e^{2}}{\epsilon_{\mathrm{in}}} + (\alpha_{eh}-\alpha_{1})(\epsilon_{\mathrm{in}}-\epsilon_{\mathrm{out}})\right]/R. \tag{A7}$$

Thus, the main effect of interparticle interactions is a redshift of the multiexciton spectra. The single-exciton threshold shifts from $\varepsilon_{g}$ to $\varepsilon_{g}-E_{\mathrm{BX}}=\varepsilon_{g}'$, the two-exciton threshold from $2\varepsilon_{g}$ to $2\varepsilon_{g}-2E_{\mathrm{BX}}=2\varepsilon_{g}'$, and the $n$-exciton threshold from $n\varepsilon_{g}$ to $n\varepsilon_{g}'$. In these conditions, the plot of the multiexciton spectra versus $h\nu/\varepsilon_{g}'$ is exactly the same as in the independent particle approximation because everything is scaled by the same quantity $\varepsilon_{g}'$.

We conclude that the results of the paper are not influenced by the main contributions to the Coulomb interactions and more generally by any correction to the total excitation energy, which is directly proportional to the number $n$ of excitons. Corrections which do not scale in direct proportion to $n$ could be induced by exchange-correlation terms by the couplings between different Slater determinants (denoted exciton-exciton interactions hereafter). However, previous calculations have shown that these terms are quite small compared to $-nE_{\mathrm{BX}}$, as well as those coming from the level dependence of the Coulomb interactions and of the self-energy shifts.[18,24–26] For $R\approx 1-2$ nm and $\epsilon_{\mathrm{in}}\approx 10$, these corrections are typically in the range of tens of meV compared to $E_{\mathrm{BX}}$ which is of the order of hundreds of meV [Eq. (A7)]. The magnitude of the exciton-exciton corrections is also confirmed by several experimental results. The biexciton binding energy, which is the difference between single-exciton and biexciton emission energies, is typically measured in the region of tens of meV.[31–34] Recently, the $P$-$P$ emission from triexciton states has been observed by several groups in CdSe nanocrystals.[34–36] This emission is found blueshifted with respect to the single-exciton $P$-$P$ transition measured by

optical absorption, but the shift is typically between 50 and 100 meV, as confirmed by theoretical calculations.[37]

Now, we estimate the effect of these exciton-exciton interactions on the parameters $\gamma_n$ used to fit the average multiplicity $\langle \tilde{N}_x(h\nu) \rangle$ on the experimental MEG yield in the case of PbSe nanocrystals.[4] We assume a biexciton binding energy of 30 meV, which is probably an upper value taking into account the large dielectric constant of PbSe ($\epsilon_\infty = 23$).[20] We simply apply a rigid redshift of 30 meV to the biexciton spectral density $N_2(h\nu)$, keeping $\varepsilon_g$ constant (or equivalently $\varepsilon_g'$ as discussed above). A redshift of $2 \times 30 = 60$ meV is considered in the case of $N_3(h\nu)$, which is consistent with the values reported for the triexcitons in CdSe nanocrystals.[34–36] Similarly, we apply redshifts of 90, 120, and 150 meV to four, five, and six-exciton spectral densities, respectively. Using $\gamma_2 = 0.007$, $\gamma_3 = 0.015$, $\gamma_4 = 1$, $\gamma_5 = 1200$, and $\gamma_6 = 3 \times 10^7$, we obtain once again an excellent fit to the experimental MEG yield, like in Fig. 6(a). The values of $\gamma_n$ are modified compared to those reported in Table II but the magnitudes remain the same, strengthening our previous conclusions. In particular, the high values of $\gamma_5$ and $\gamma_6$ remain unrealistic.

## APPENDIX B: SPECTRAL DENSITIES OF MULTIEXCITON STATES IN A MODEL SYSTEM

We consider a simple model, in which the density of single-particle states is a constant $N_c$ in the conduction band and $N_v$ in the valence band (confinement effects are neglected). From Eq. (3), the spectral densities of multiexciton states are given by

$$N_1(h\nu) = N_c N_v (h\nu - \varepsilon_g), \tag{B1}$$

$$N_2(h\nu) = \frac{(N_c N_v)^2}{24} (h\nu - 2\varepsilon_g)^3, \tag{B2}$$

$$N_3(h\nu) = \frac{(N_c N_v)^3}{4320} (h\nu - 3\varepsilon_g)^5, \tag{B3}$$

$$N_4(h\nu) = \frac{(N_c N_v)^4}{2\,903\,040} (h\nu - 4\varepsilon_g)^7, \tag{B4}$$

$$N_5(h\nu) = \frac{(N_c N_v)^5}{5\,225\,472\,000} (h\nu - 5\varepsilon_g)^9, \tag{B5}$$

$$N_6(h\nu) \approx \frac{(N_c N_v)^6}{2.069\,286\,912 \times 10^{13}} (h\nu - 6\varepsilon_g)^{11}. \tag{B6}$$

These expressions explain the rapid variation of the spectral densities with $h\nu$ over several orders of magnitude.

*christophe.delerue@isen.fr


[1] R. D. Schaller and V. I. Klimov, Phys. Rev. Lett. **92**, 186601 (2004).
[2] A. J. Nozik, Annu. Rev. Phys. Chem. **52**, 193 (2001).
[3] R. J. Ellingson, M. C. Beard, J. C. Johnson, P. Yu, O. I. Micic, A. J. Nozik, A. Shabaev, and A. L. Efros, Nano Lett. **5**, 865 (2005).
[4] R. D. Schaller, V. M. Agranovitch, and V. I. Klimov, Nat. Mater. **1**, 189 (2005).
[5] R. D. Schaller, M. A. Petruska, and V. I. Klimov, Appl. Phys. Lett. **87**, 253102 (2005).
[6] R. D. Schaller, M. Sykora, S. Jeong, and V. I. Klimov, J. Phys. Chem. B **110**, 25332 (2006).
[7] J. J. H. Pijpers, E. Hendry, M. T. W. Milder, R. Fanciulli, J. Savolainen, J. L. Herek, D. Vanmaekelbergh, S. Ruhman, D. Mocatta, D. Oron, A. Aharoni, U. Banin, and M. Bonn, J. Phys. Chem. C **111**, 4146 (2007).
[8] R. D. Schaller, J. M. Pietryga, and V. I. Klimov, Nano Lett. **7**, 3469 (2007).
[9] M. C. Beard, K. P. Knutsen, P. Yu, J. M. Luther, Q. Song, W. K. Metzger, R. J. Ellingson, and A. J. Nozik, Nano Lett. **7**, 2506 (2007).
[10] G. Nair and M. G. Bawendi, Phys. Rev. B **76**, 081304(R) (2007).
[11] B. L. Wehrenberg, C. Wang, and P. Guyot-Sionnest, J. Phys. Chem. B **106**, 10634 (2002).
[12] R. D. Schaller, J. M. Pietryga, S. V. Goupalov, M. A. Petruska, S. A. Ivanov, and V. I. Klimov, Phys. Rev. Lett. **95**, 196401 (2005).
[13] T. Okuno, Y. Masumoto, M. Ikezawa, T. Ogawa, and A. A. Lipovskii, Appl. Phys. Lett. **77**, 504 (2000).
[14] J. M. Harbold, H. Du, T. D. Krauss, K.-S. Cho, C. B. Murray, and F. W. Wise, Phys. Rev. B **72**, 195312 (2005).
[15] G. Allan and C. Delerue, Phys. Rev. B **73**, 205423 (2006).
[16] A. Franceschetti, J. M. An, and A. Zunger, Nano Lett. **6**, 2191 (2006).
[17] A. Shabaev, A. L. Efros, and A. J. Nozik, Nano Lett. **6**, 2856 (2006).
[18] C. Delerue and M. Lannoo, *Nanostructures: Theory and Modelling* (Springer-Verlag, Berlin, 2004).
[19] R. D. Schaller and V. I. Klimov, Phys. Rev. Lett. **96**, 097402 (2006).
[20] G. Allan and C. Delerue, Phys. Rev. B **70**, 245321 (2004).
[21] Y. M. Niquet, C. Delerue, G. Allan, and M. Lannoo, Phys. Rev. B **65**, 165334 (2002).
[22] Y. M. Niquet, C. Delerue, G. Allan, and M. Lannoo, Phys. Rev. B **62**, 5109 (2000).
[23] V. I. Rupasov and V. I. Klimov, Phys. Rev. B **76**, 125321 (2007).
[24] E. Martin, C. Delerue, G. Allan, and M. Lannoo, Phys. Rev. B **50**, 18258 (1994).
[25] J. Shumway, A. Franceschetti, and A. Zunger, Phys. Rev. B **63**, 155316 (2001).
[26] M. Califano, A. Franceschetti, and A. Zunger, Phys. Rev. B **75**, 115401 (2007).
[27] Y. Kayanuma, Solid State Commun. **59**, 405 (1986).
[28] C. Delerue, M. Lannoo, and G. Allan, Phys. Rev. Lett. **84**, 2457 (2000); **89**, 249901(E) (2002).
[29] L. E. Brus, J. Chem. Phys. **79**, 5566 (1983); **80**, 4403 (1984).
[30] M. Lannoo, C. Delerue, and G. Allan, Phys. Rev. Lett. **74**, 3415

(1995).
[31] K. I. Kang, A. D. Kepner, S. V. Gaponenko, S. W. Koch, Y. Z. Hu, and N. Peyghambarian, Phys. Rev. B **48**, 15449 (1993).
[32] M. Achermann, J. A. Hollingsworth, and V. I. Klimov, Phys. Rev. B **68**, 245302 (2003).
[33] B. Patton, W. Langbein, and U. Woggon, Phys. Rev. B **68**, 125316 (2003).
[34] J. Michel Caruge, Y. Chan, V. Sundar, H. J. Eisler, and M. G. Bawendi, Phys. Rev. B **70**, 085316 (2004).
[35] C. Bonati, M. B. Mohamed, D. Tonti, G. Zgrablic, S. Haacke, F. van Mourik, and M. Chergui, Phys. Rev. B **71**, 205317 (2005).
[36] D. Oron, M. Kazes, I. Shweky, and U. Banin, Phys. Rev. B **74**, 115333 (2006).
[37] A. Franceschetti and M. C. Troparevsky, J. Phys. Chem. C **111**, 6154 (2007).